Spectrometer – particle identification

Lecture: Hans-Jürgen Wollersheim

e-mail: h.j.wollersheim@gsi.de

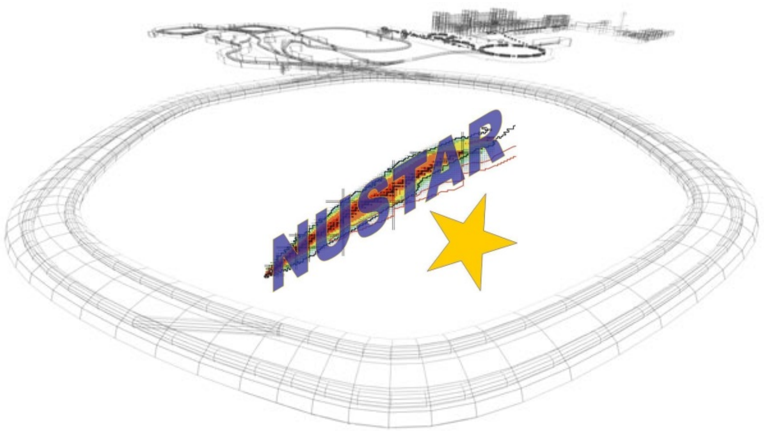

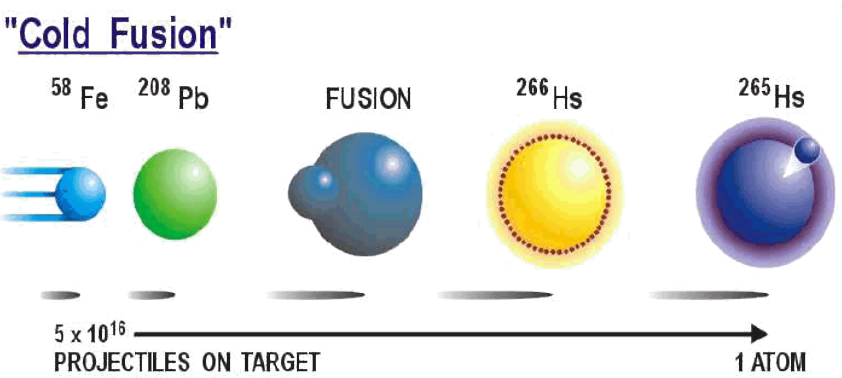

Solar abundances of elements

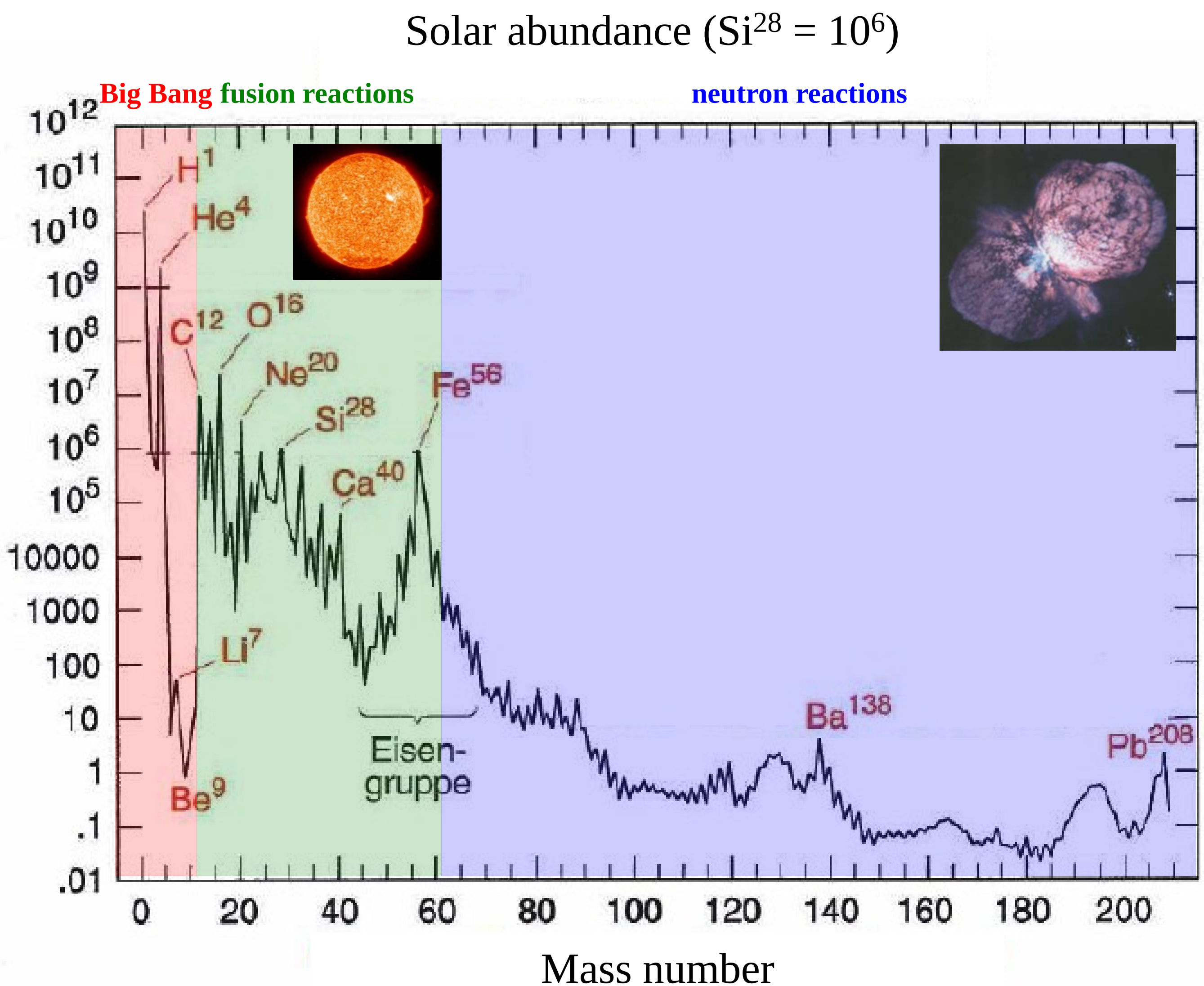

open questions:

- Why is Fe more common than Au ?
- Why do the heavy elements exist and how are they produced?
- Can we explain the solar abundances of the elements?

The chart of nuclides

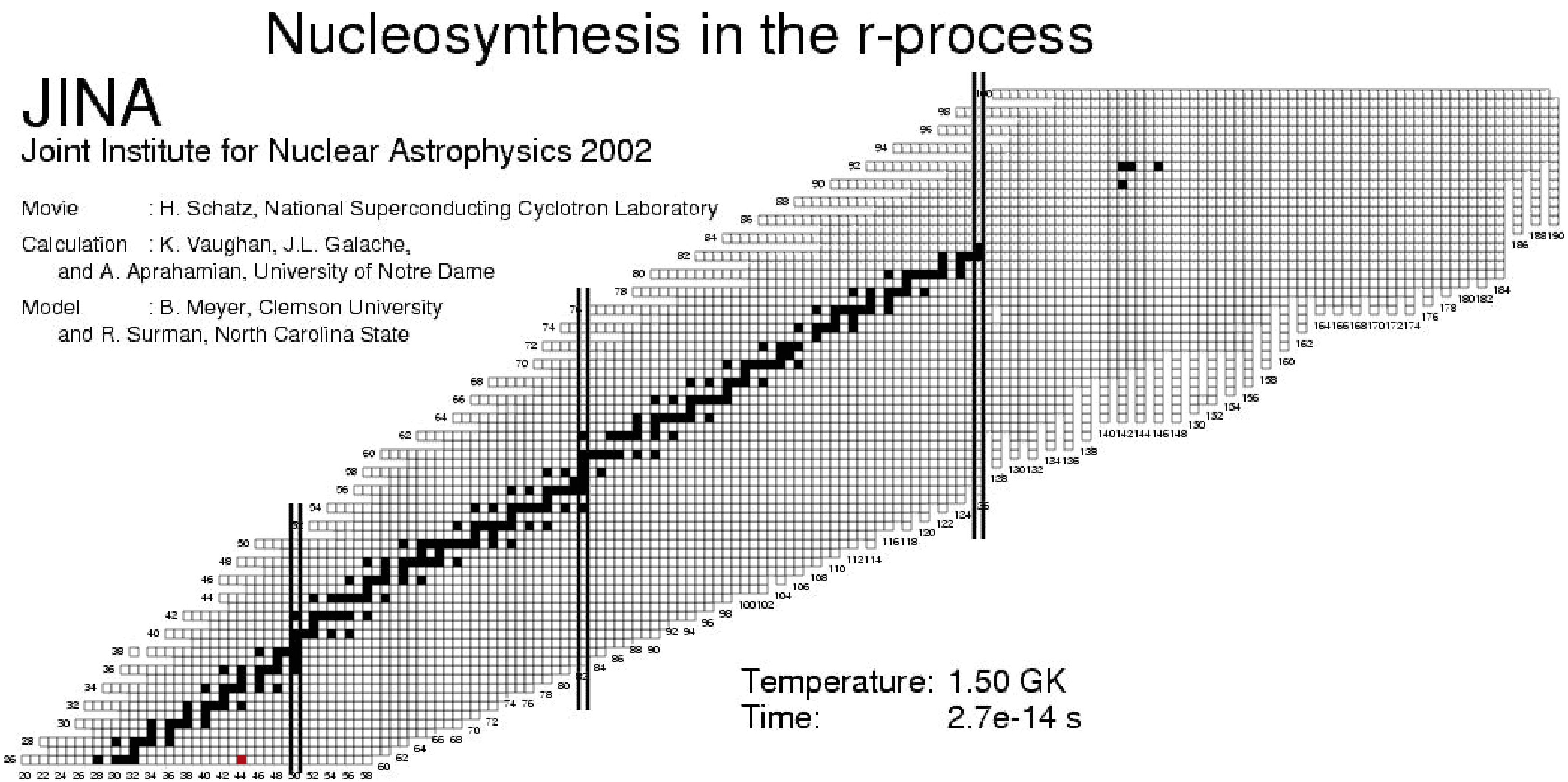

Radioactive Ion Beams at GSI

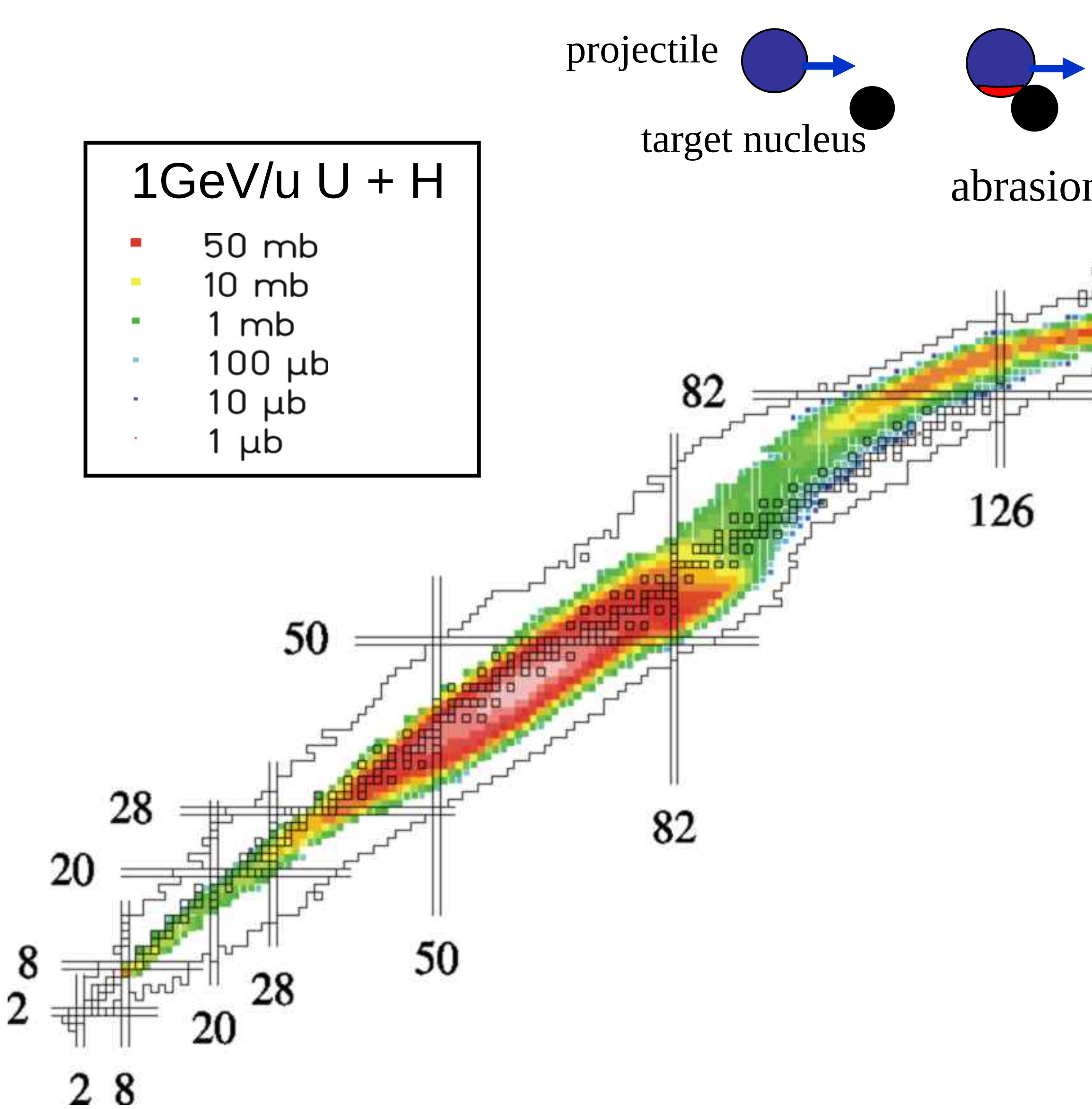

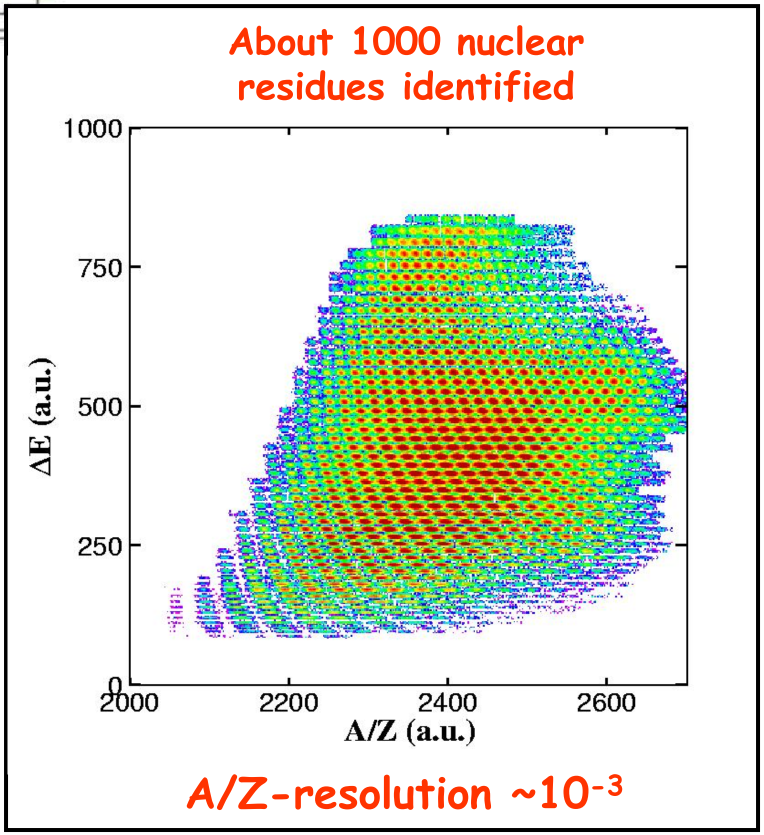

FRagment **S**eparator at GSI

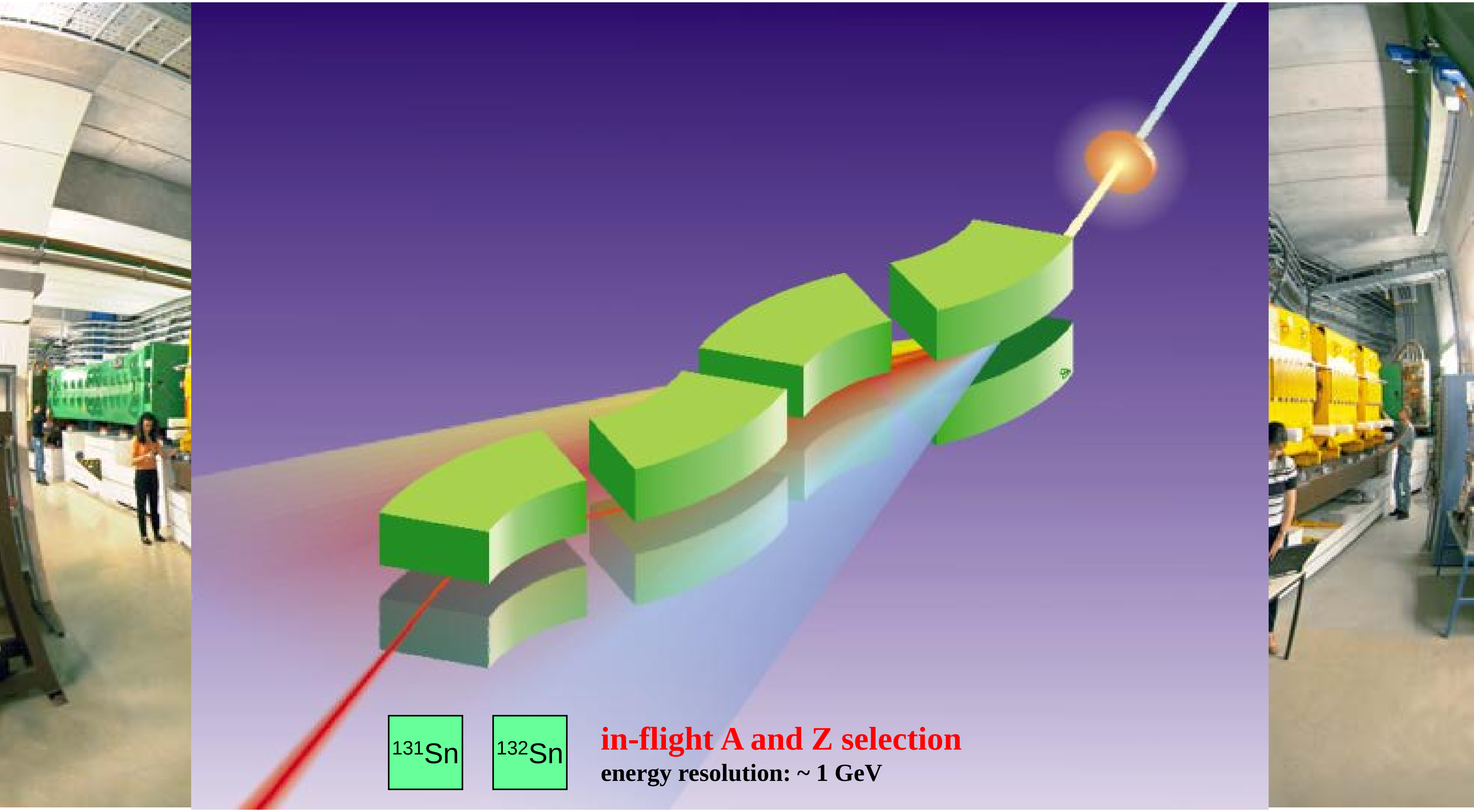

Rare Isotope Selection at FRS: $B\rho - \Delta E - B\rho$ selection

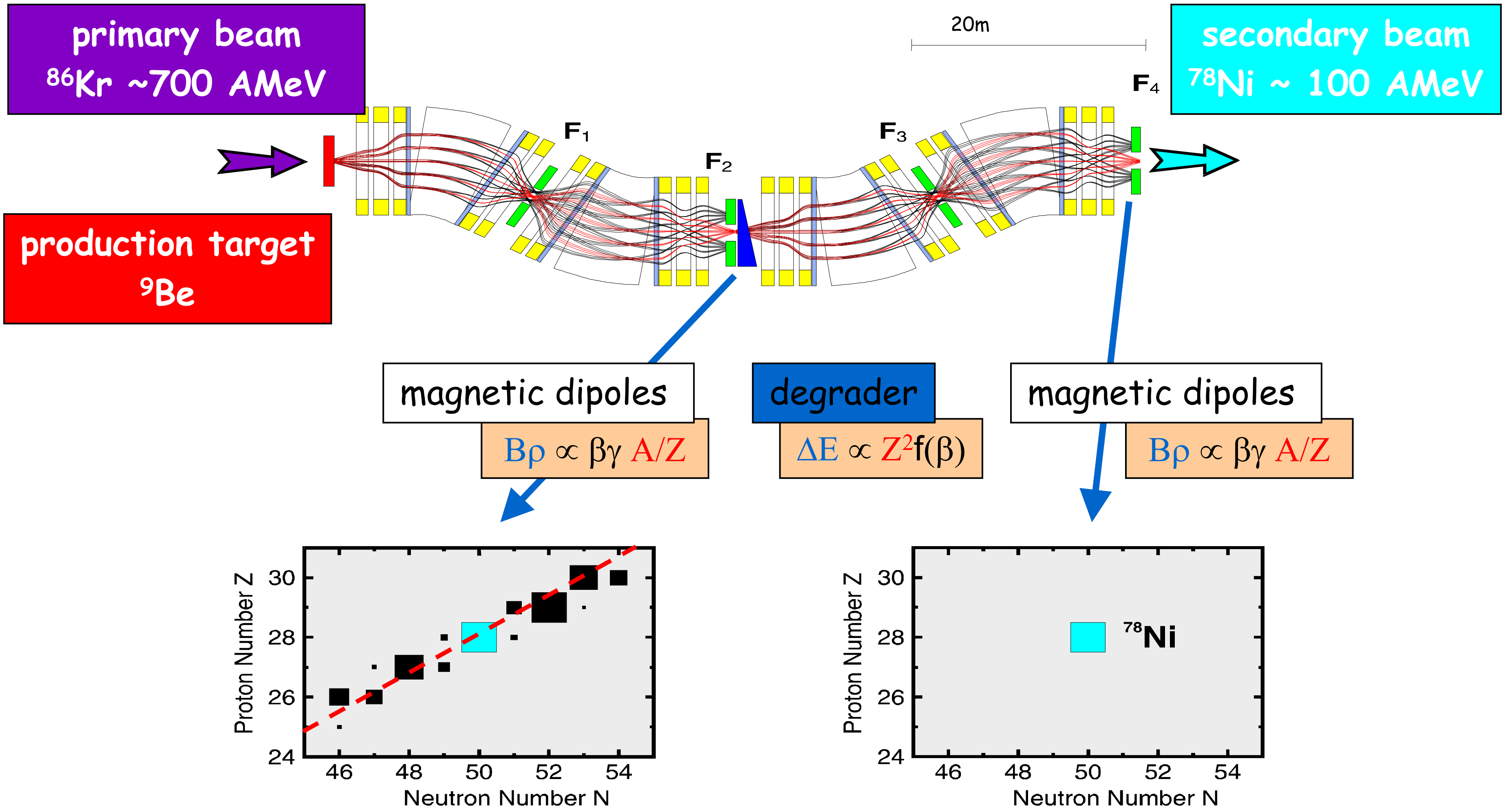

Production, Separation, Identification

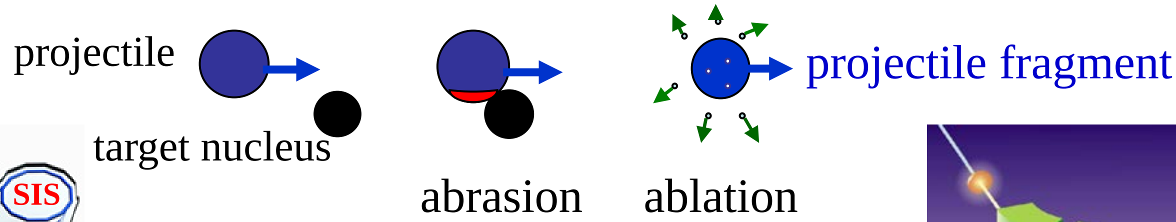

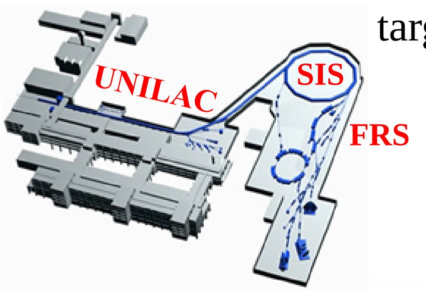

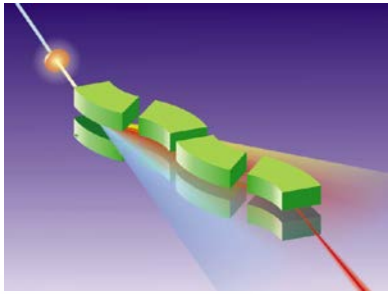

FRagment **S**eparator

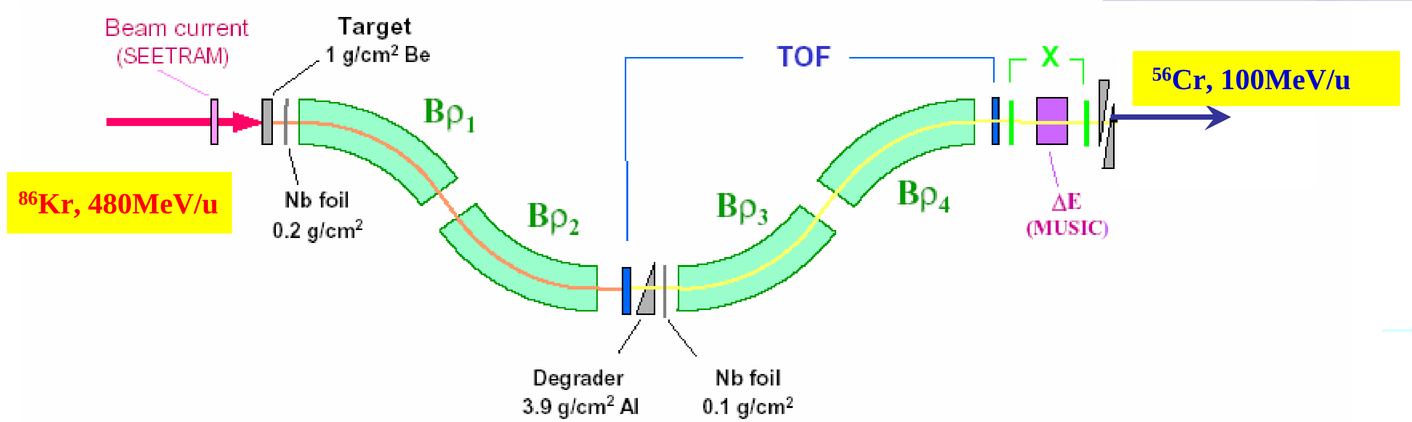

Standard FRS detectors

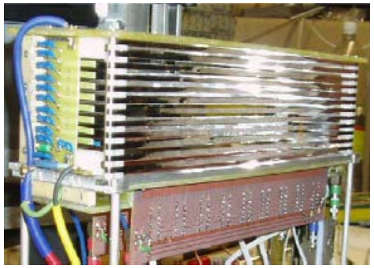

TPC-**x,y position** @ S2,S4

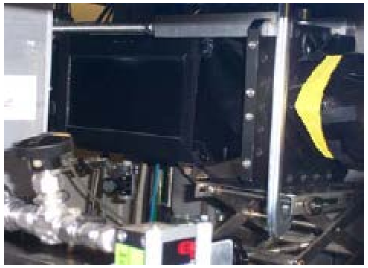

Plastic scintillator (**TOF**) @ S4

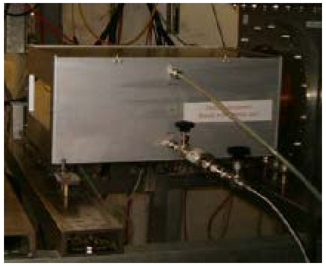

MUSIC (**ΔE**) @ S4

Production, Separation, Identification

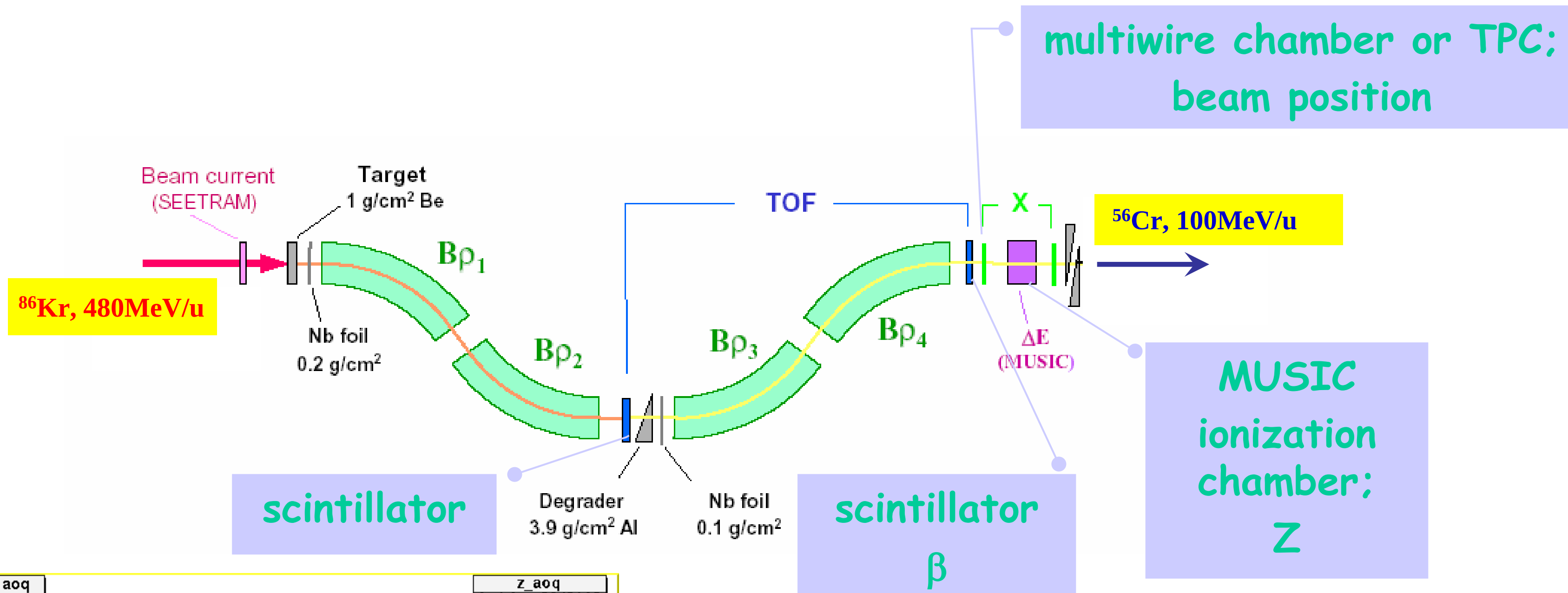

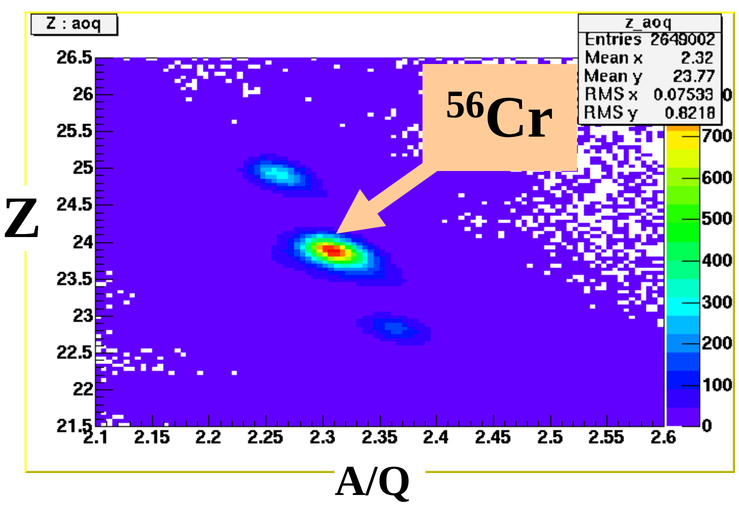

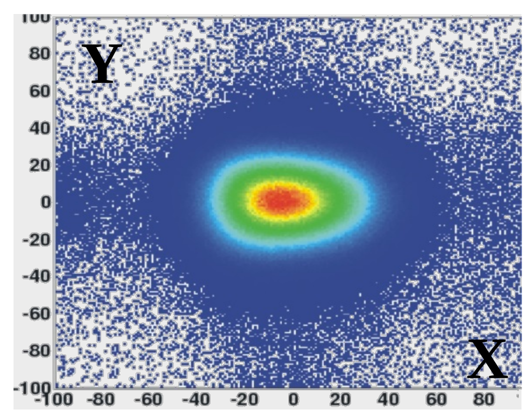

Experimental set-up for γ-ray spectroscopy

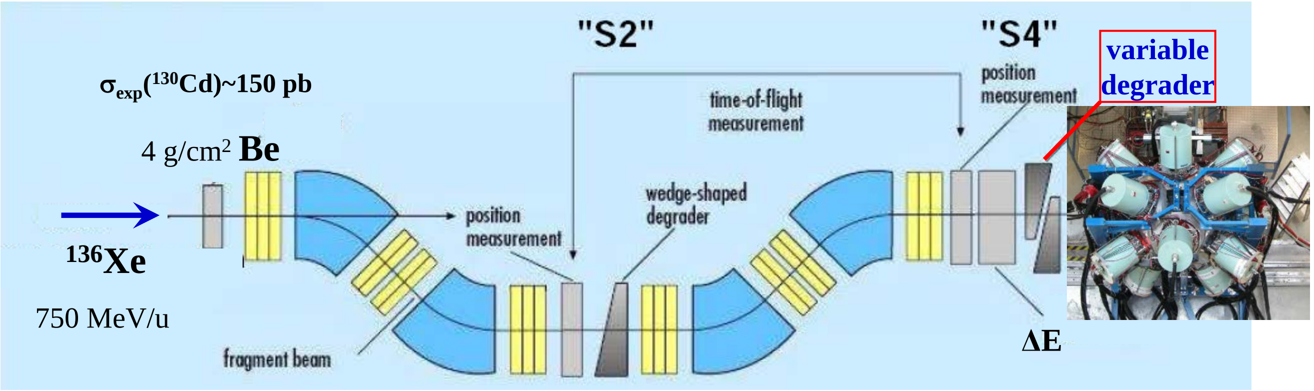

^{130}Cd

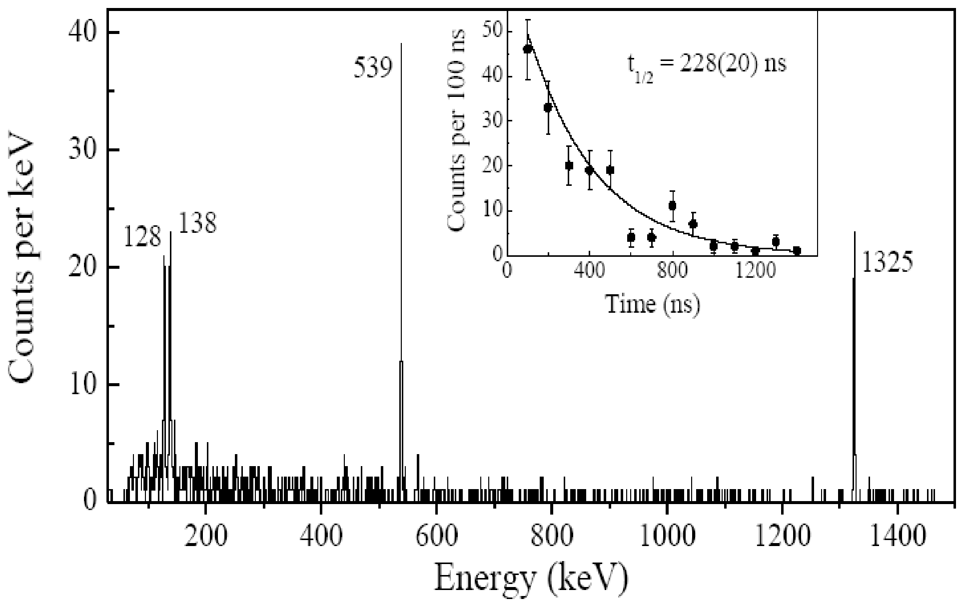

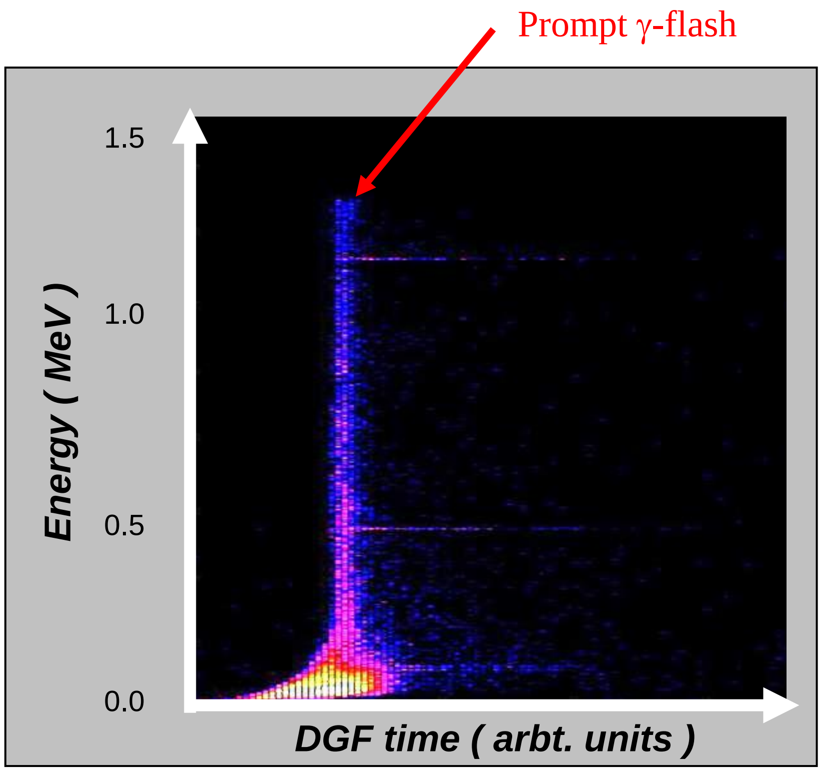

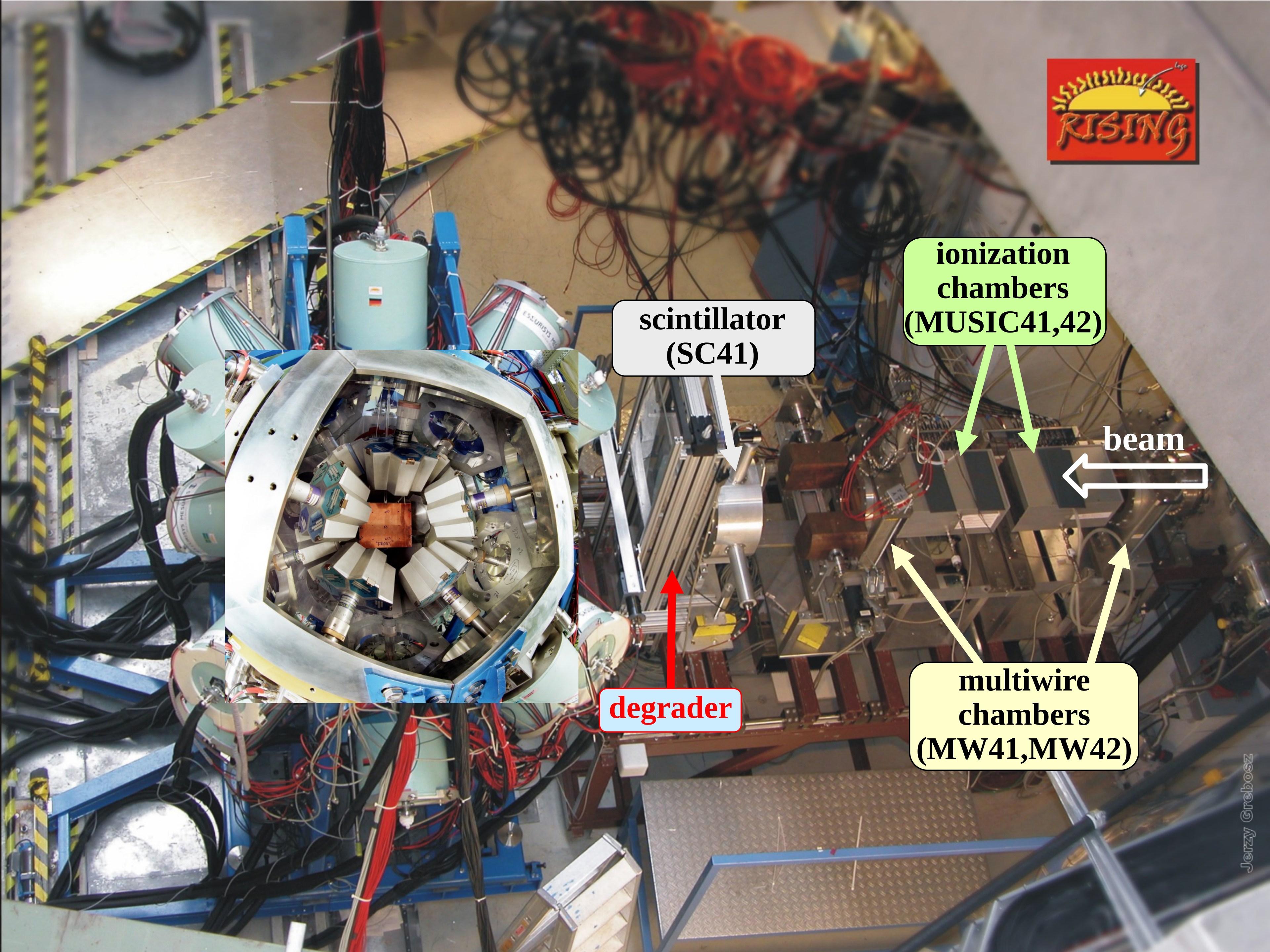
RISING
ionization chambers (MUSIC41,42)
scintillator (SC41)
beam
degrader
multiwire chambers (MW41,MW42)
Jerzy Grebosz

The astrophysical r-process ´path´

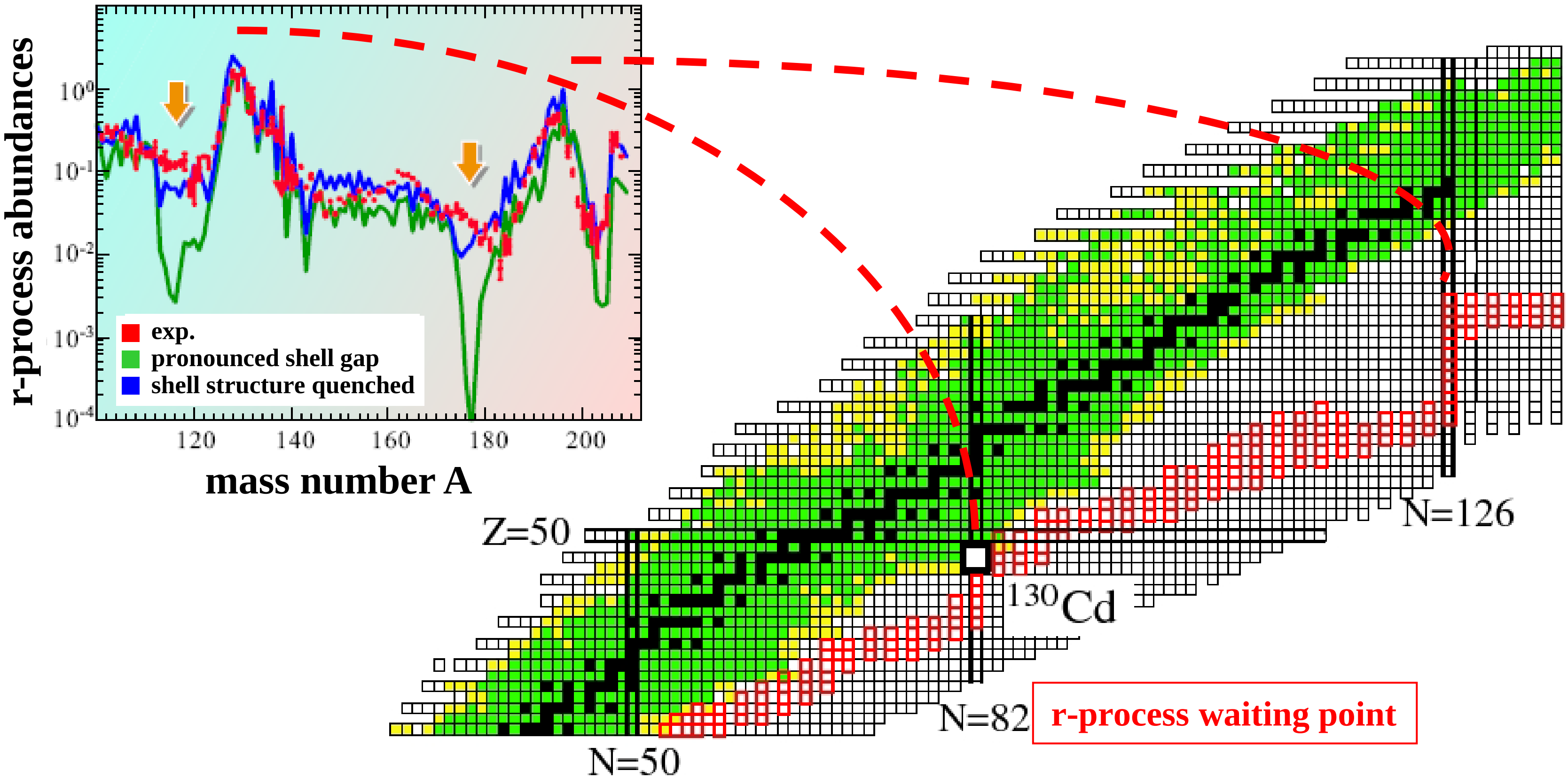

Assumption of a N=82 shell quenching leads to a considerable improvement in the global abundance fit in r-process calculations !

Reaction with Relativistic Radioactive Beams – R^{3}B

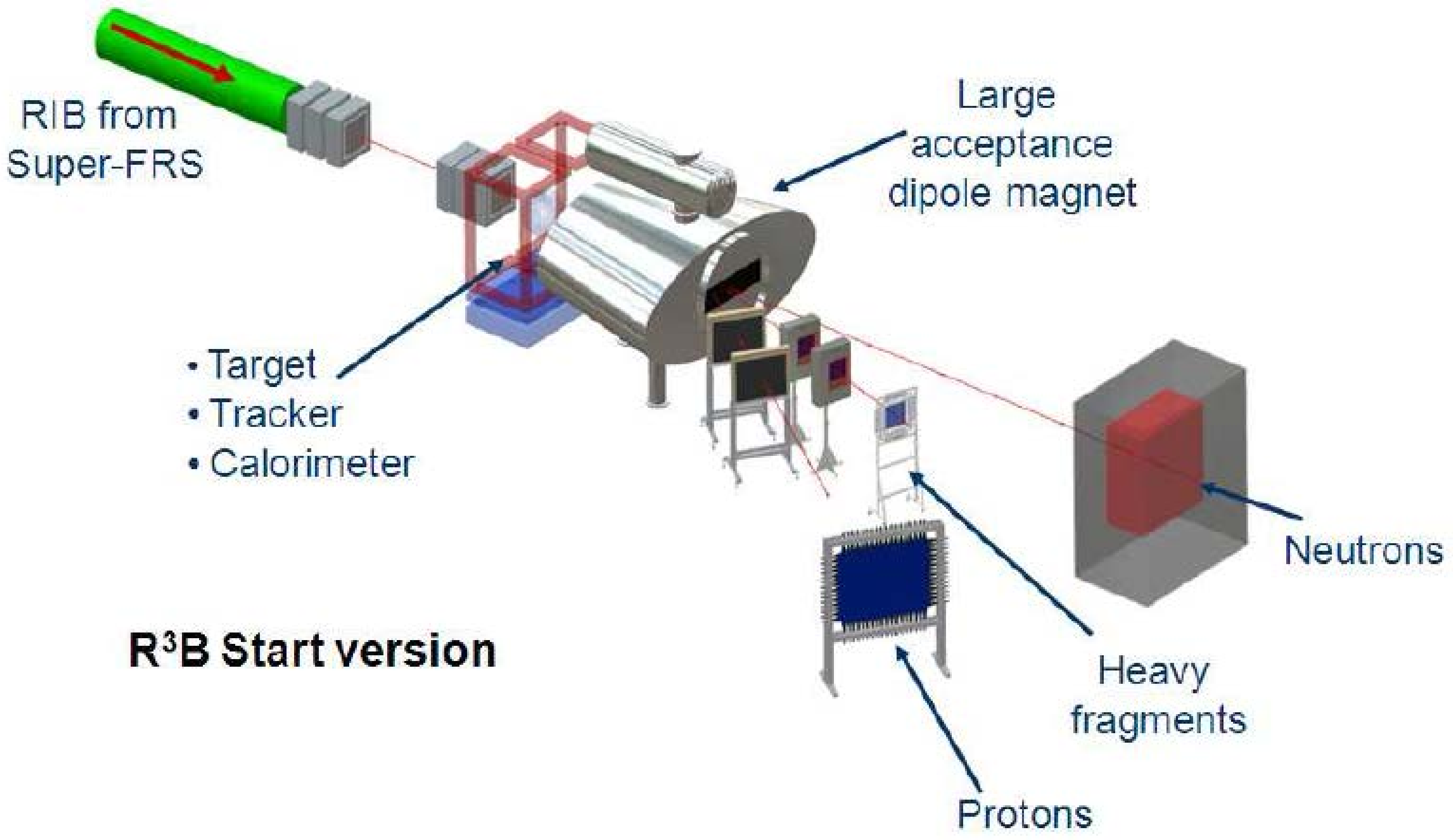

Excitation energy E* from kinematically complete measurement of all outgoing particles

$$E^* = \left(\sqrt{\sum_i m_i^2 + \sum_{i \neq j} m_i m_j \gamma_i \gamma_j \left(1 - \beta_i \beta_j cos\vartheta_{ij}\right)} - m_{proj} \right) c^2 + E_{\gamma,sum}$$

Large Area Neutron Detector

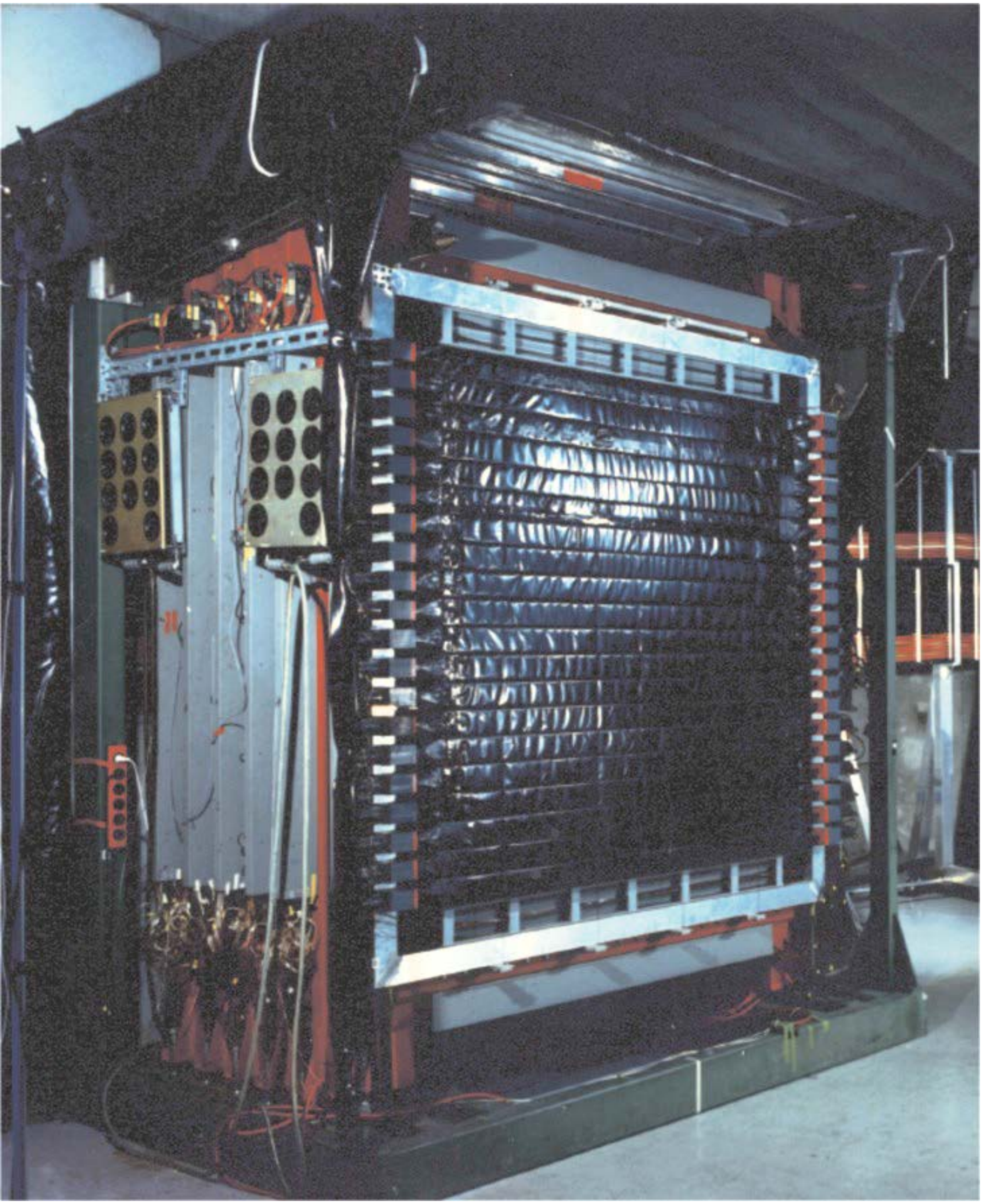

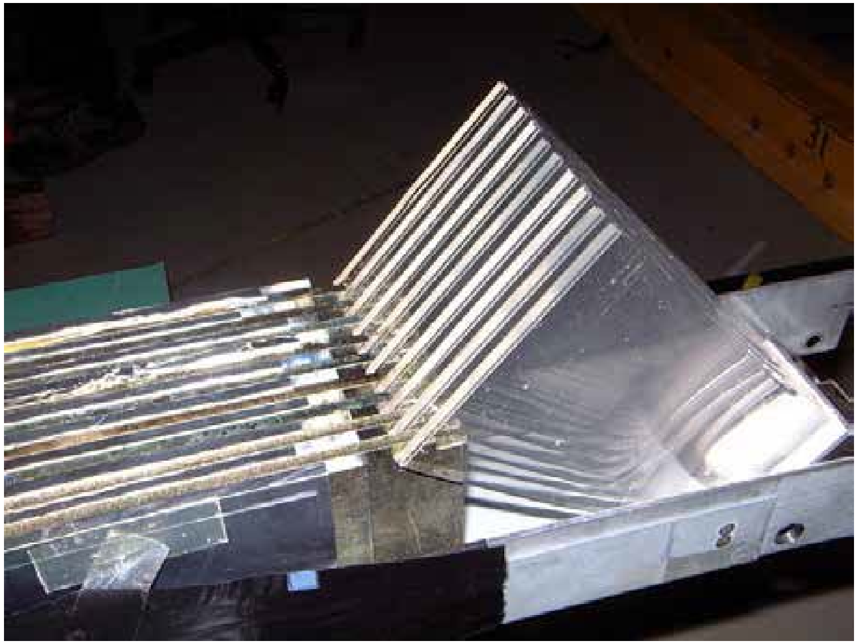

Large ***A***rea ***N***eutron ***D***etector (2m x 2m x 1m)

- neutron energy $T_n \leq 1$ GeV
- $\Delta T_n/T_n = 5.3\%$
- efficiency ~1
- passive Fe-converter

Dipole strength distribution of ^{68}Ni

mean field calculation

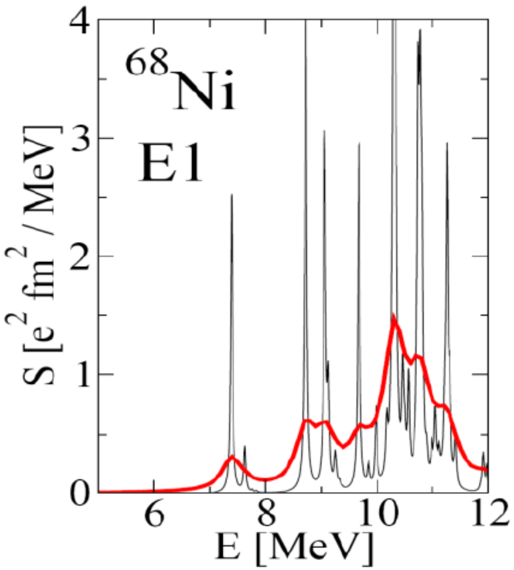

E.Litvinova et al.; PRC 79, (2009) 054312

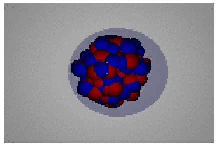

Pygmy resonance

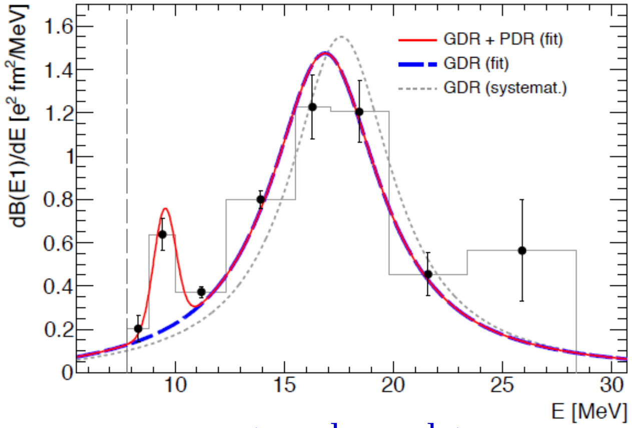

neutron decay data

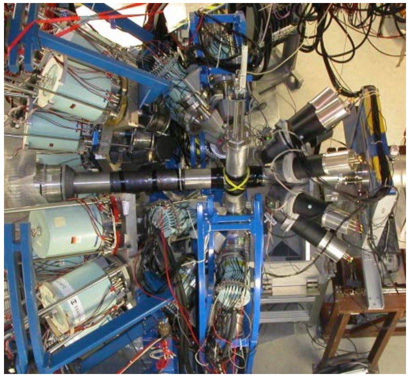

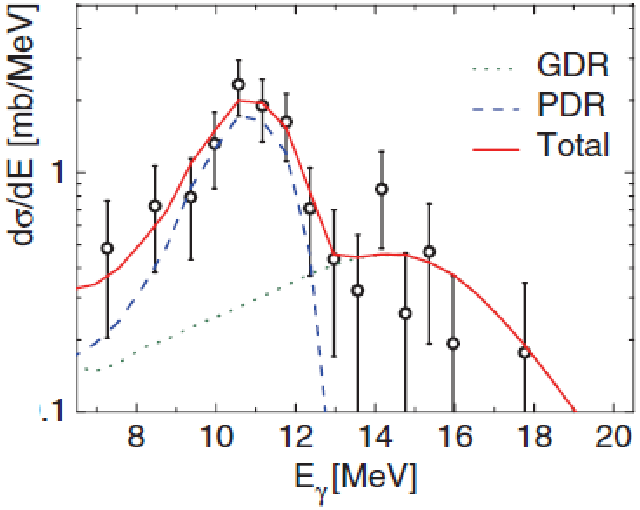

γ-ray decay data

direct γ-decay branching ratio:

$\Gamma_0/\Gamma = 7(2)\%$

O. Wieland et al.; Phys. Rev. Lett 102, 092502 (2009)

D. Rossi et al.; Phys. Rev. Lett 111, 242503 (2013)

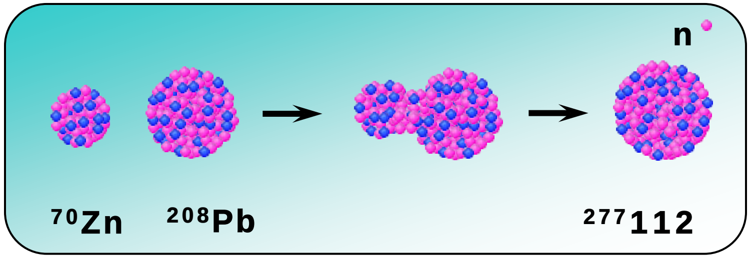

Fusion

$\frac{1}{10^{12}}$

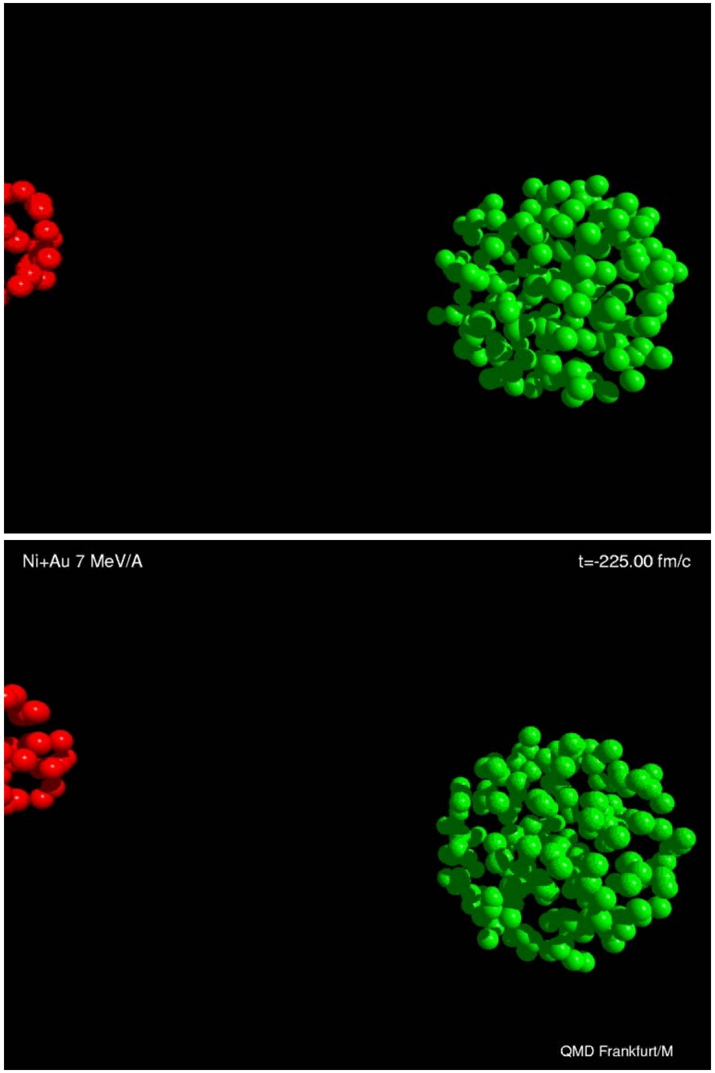

Separator for Heavy Ion Products (SHIP)

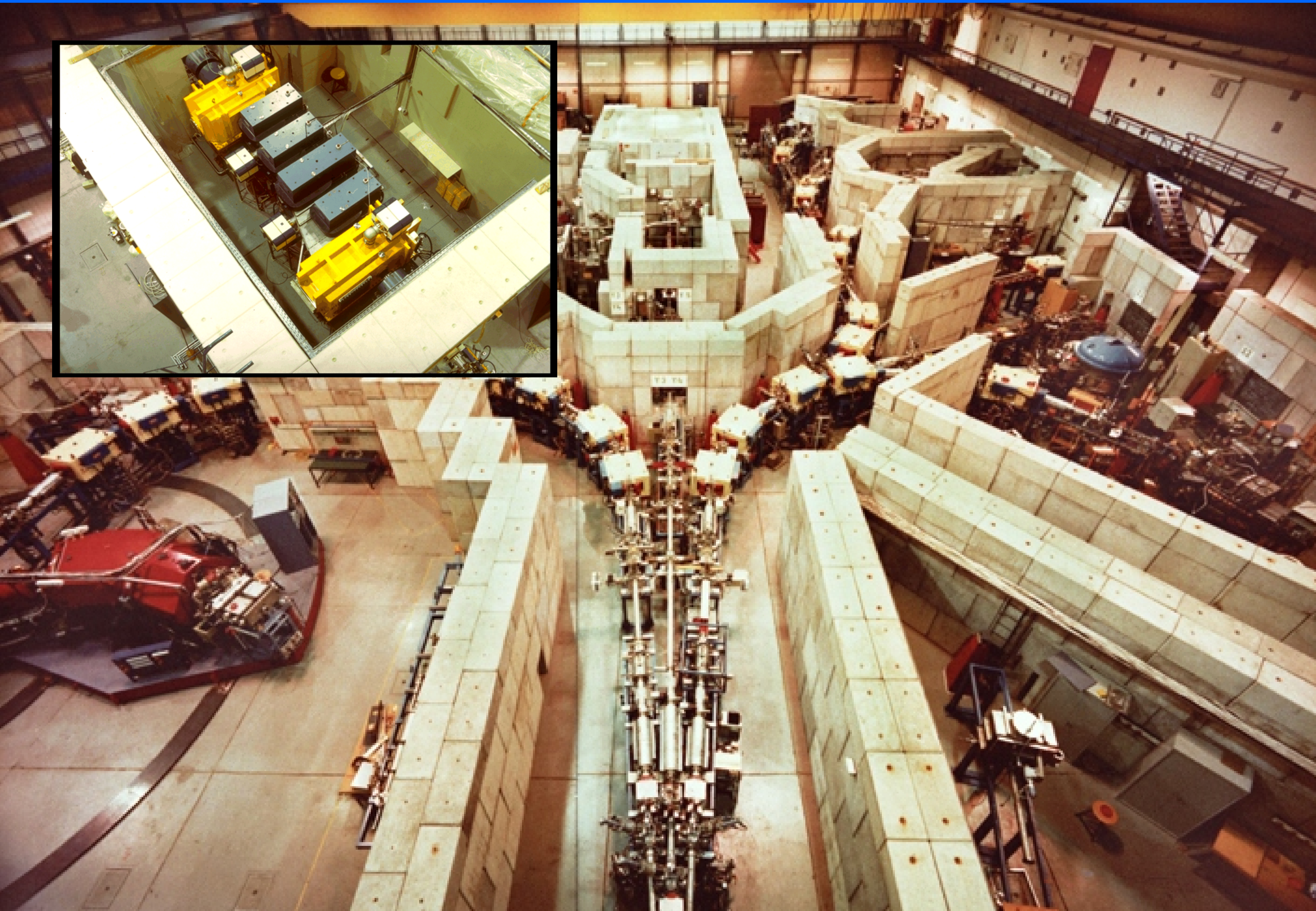

Separator for Heavy Ion Products (SHIP)

- Fusion products are slower than scattered or transfer particles

$$v_{CN} = [m_p/(m_p + m_t)] \cdot v_p$$

$$e.q.\, v_p \approx 10.3\% \quad \rightarrow \quad v_{CN} \approx 2.2\%$$

- E- and B-field are perpendicular to each other

$$B \cdot \rho = \frac{m \cdot v}{e \cdot q}$$

$$E \cdot \rho = \frac{m \cdot v^2}{e \cdot q}$$

$$F_{mag} = F_{el} \Rightarrow F_{tot} = 0$$

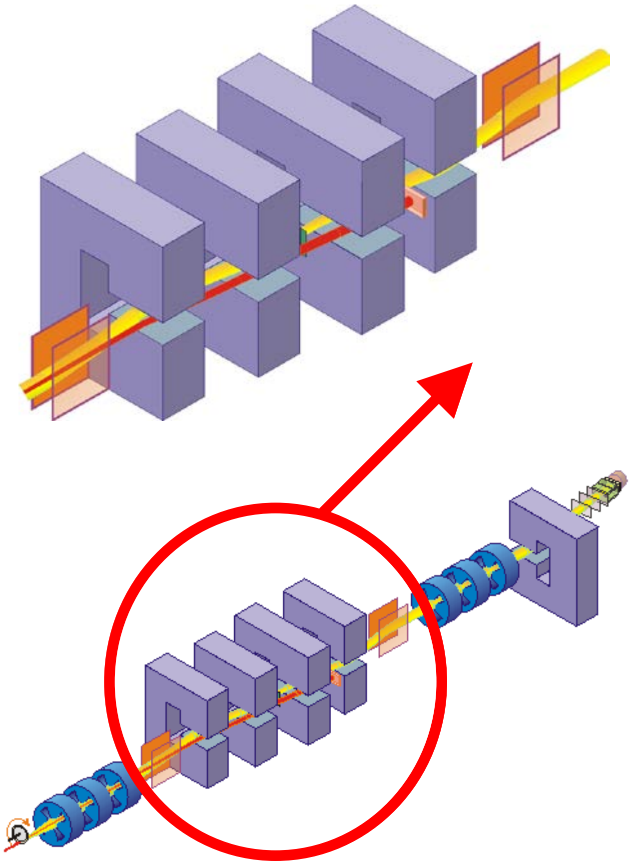

electric deflectors: ±330 kV   dipole magnets: 0.7 T max

Separator for Heavy Ion Products (SHIP)

- The choice of E and B determines the transmitted velocity

$$v = \frac{E}{B}$$

- The rejected beam will be stopped on a cooled Cu plate

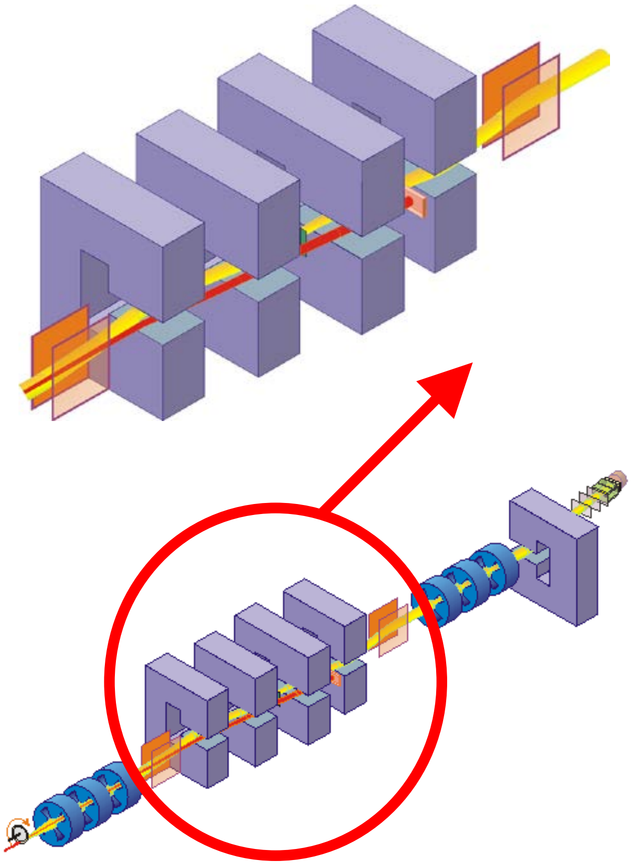

SHIP – stop detector

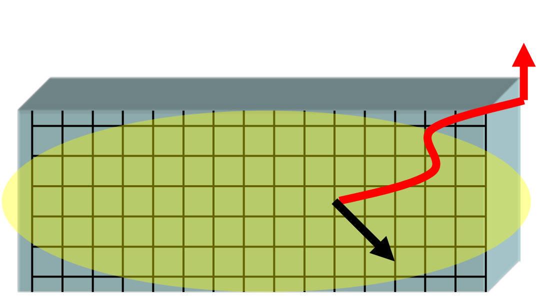

SHE will be measured in a pixel

Wait for the emission of an α-particle
(or β-particle)

correlation method: implantation and decay event in the same pixel

- position sensitive Silicon detector determines the position an energy of SHE and α, β, ...

area: 27*87mm², thickness: 0.3mm, 16 strips
energy resolution ΔE=18-20 keV @ E_{α}> 6MeV (cooling 260K)
position resolution Δx=0.3mm (FWHM)

Synthesis and identification of heavy elements with SHIP

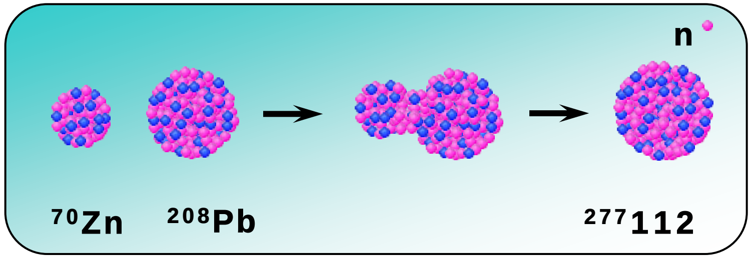

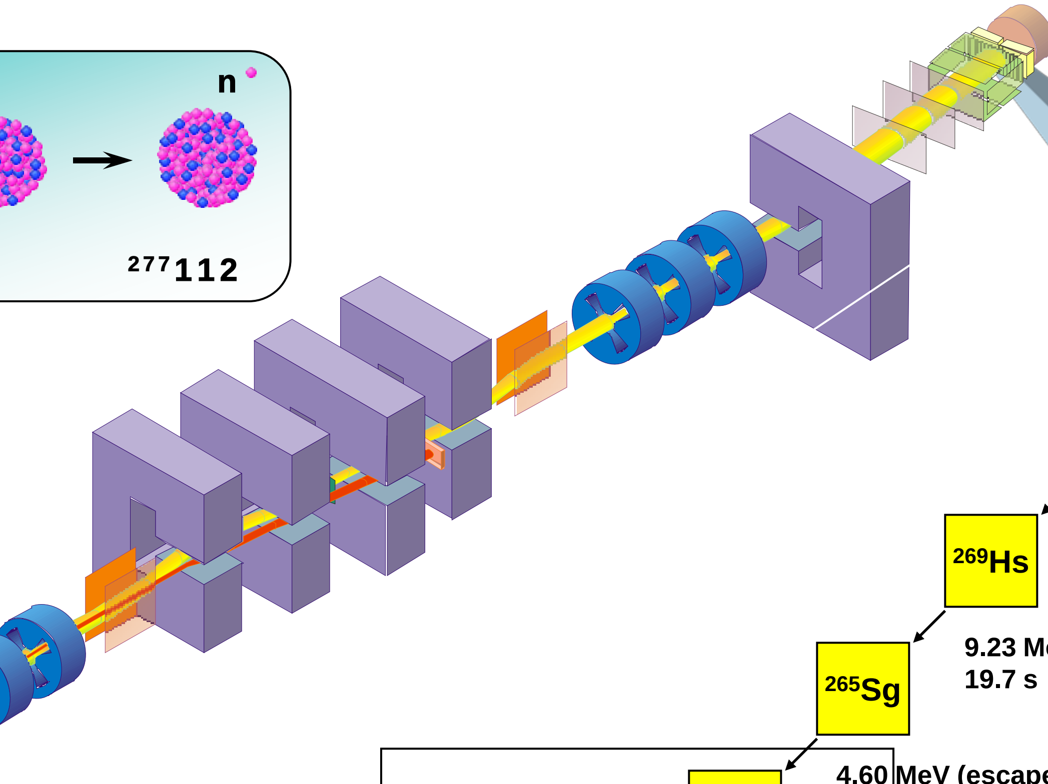

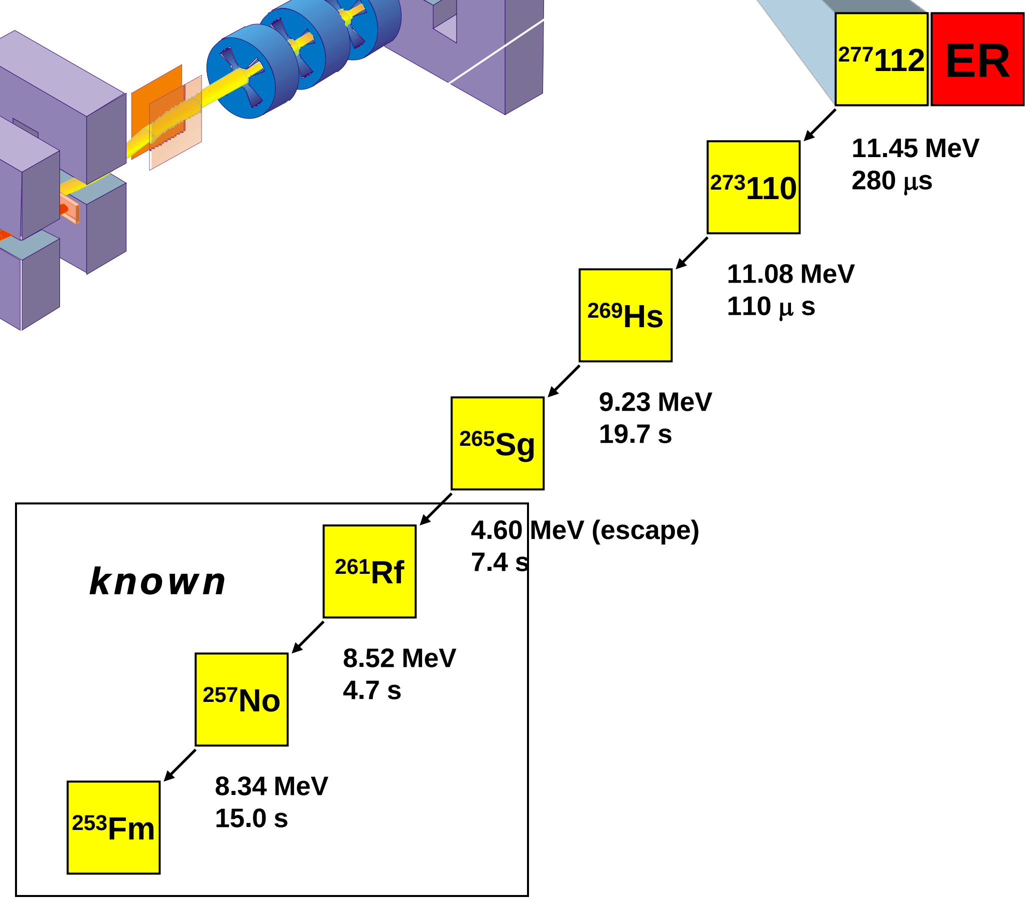

Date: 09-Feb-1996
Time: 22:37 h

kinematical separation (in flight)

using electric deflectors
and dipole magnets

$v = E/B$ → *velocity filter*

Synthesis and identification of heavy elements with SHIP

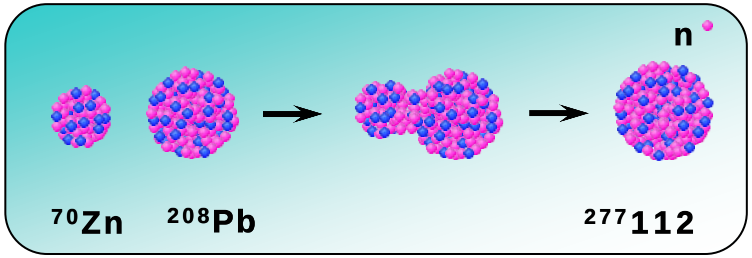

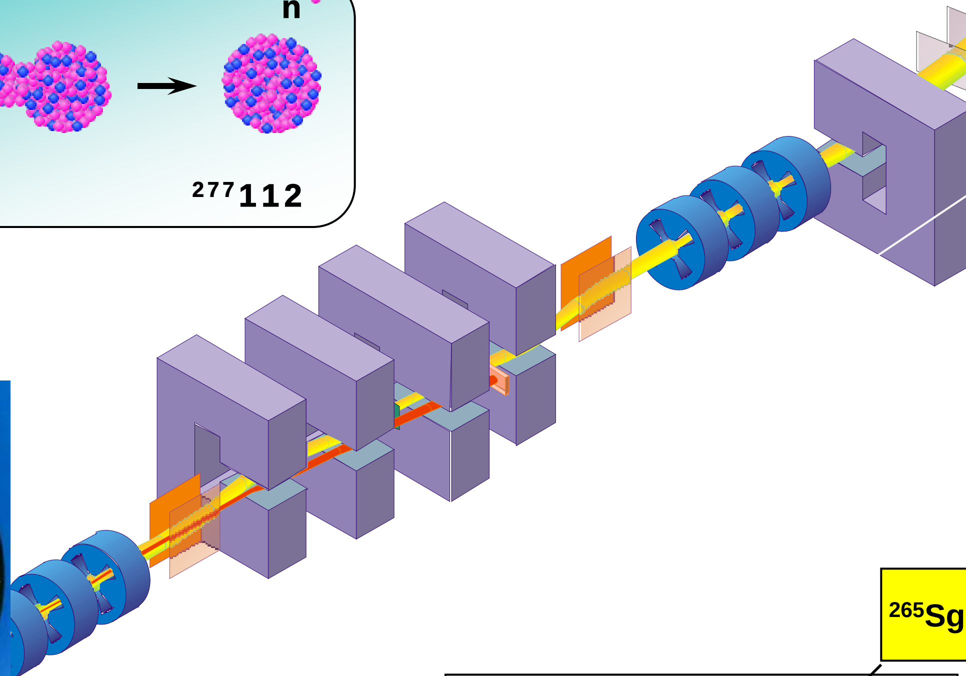

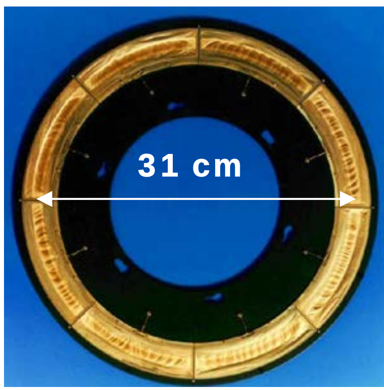

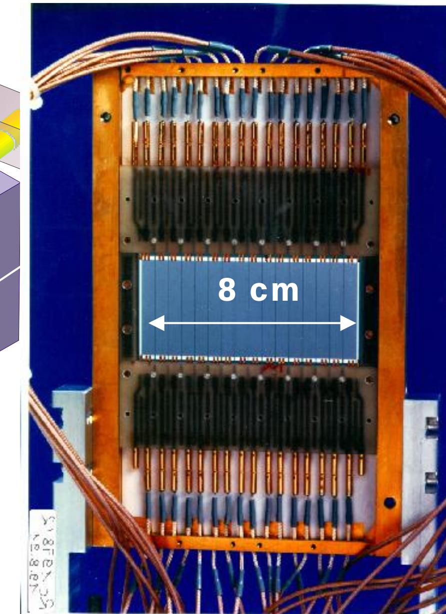

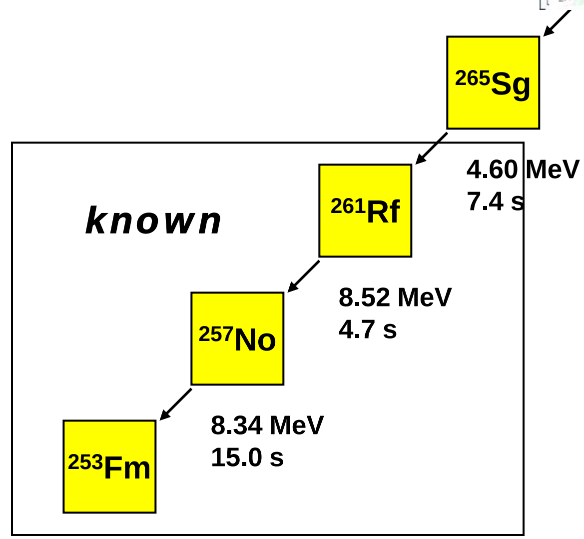

Date: 09-Feb-1996
Time: 22:37 h

Identification by α-α correlations down to ***known*** *isotopes*

kinematical separation (in flight)

using electric deflectors and dipole magnets

$v = E/B$ → *velocity filter*

Cherenkov Radiation Threshold Detection - The Kaon Spectrometer

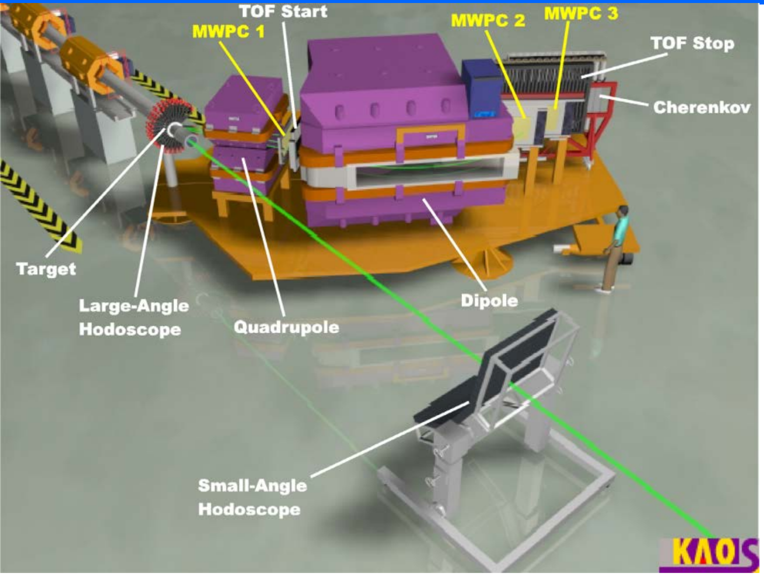

Experimental task is to identify the kaons in a large background of protons and pions.

$p^+, \pi^+, K^+ \; rate: \quad \sim 10000/1000/1$

- Time-of-flight (ToF) measurement

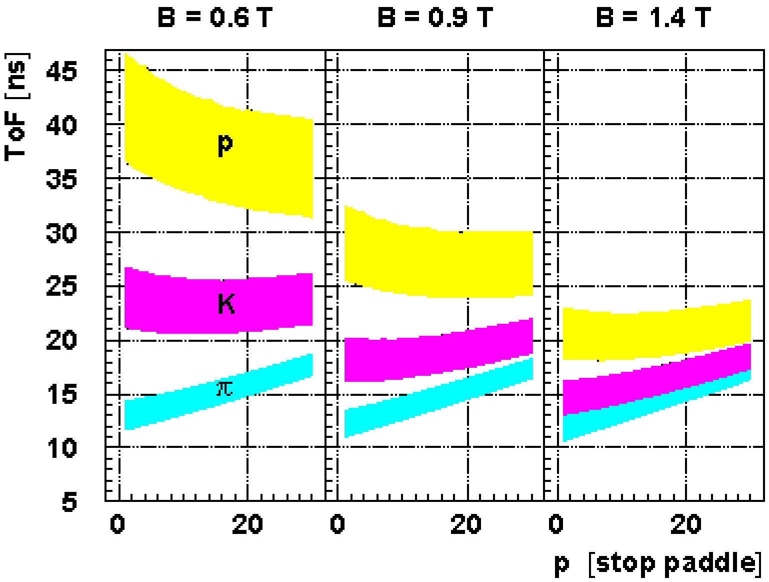

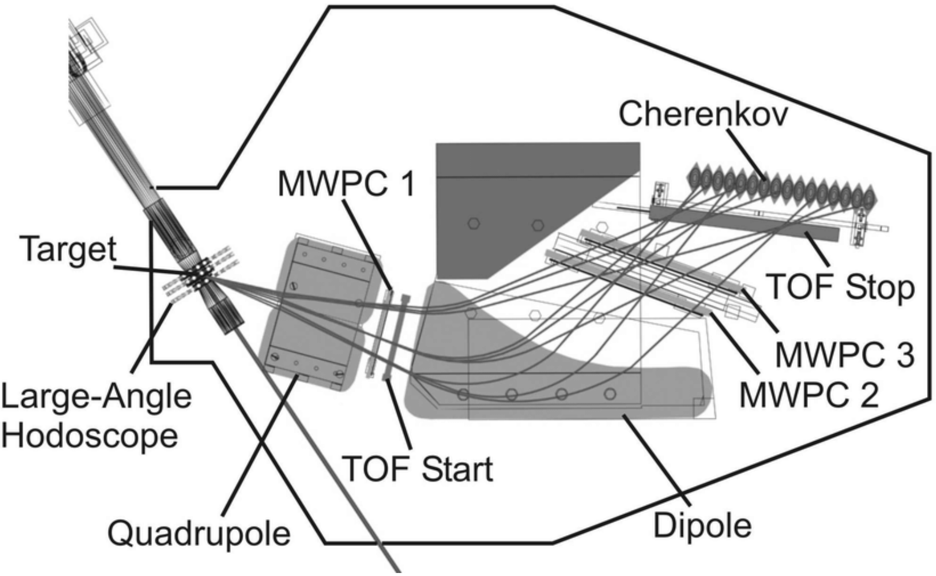

Cherenkov Radiation Threshold Detection - The Kaon Spectrometer

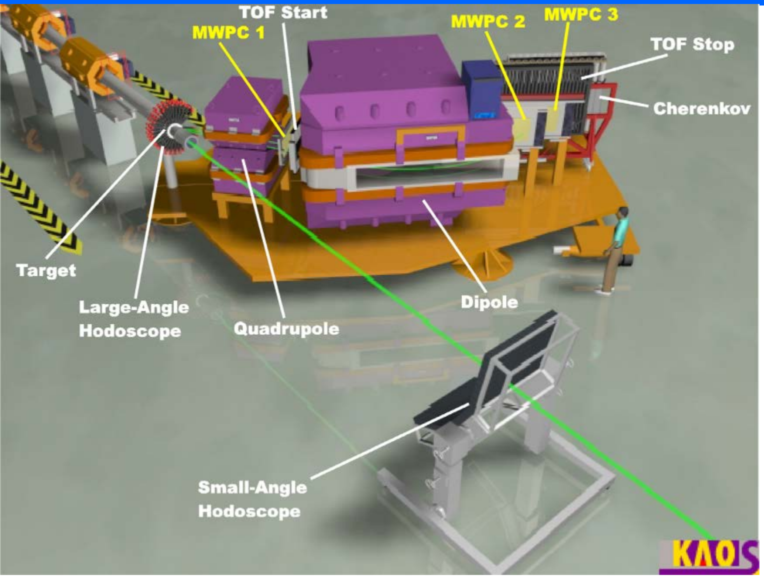

Experimental task is to identify the kaons in a large background of protons and pions.

$p^+, \pi^+, K^+ \, rate: \quad \sim 10000/1000/1$

- Time-of-flight (ToF) measurement
- Cherenkov detectors
  1) lucite ($n = 1.49, \beta \geq 0.67$) and water ($n = 1.34, \beta \geq 0.75$) i.e. above the velocity of protons for $p < 0.8\ GeV/c$ and $p < 1\ GeV/c$ respectively
  2) silica aerogel ($n = 1.05, \beta \geq 0.95$) allows separation of pions and kaons

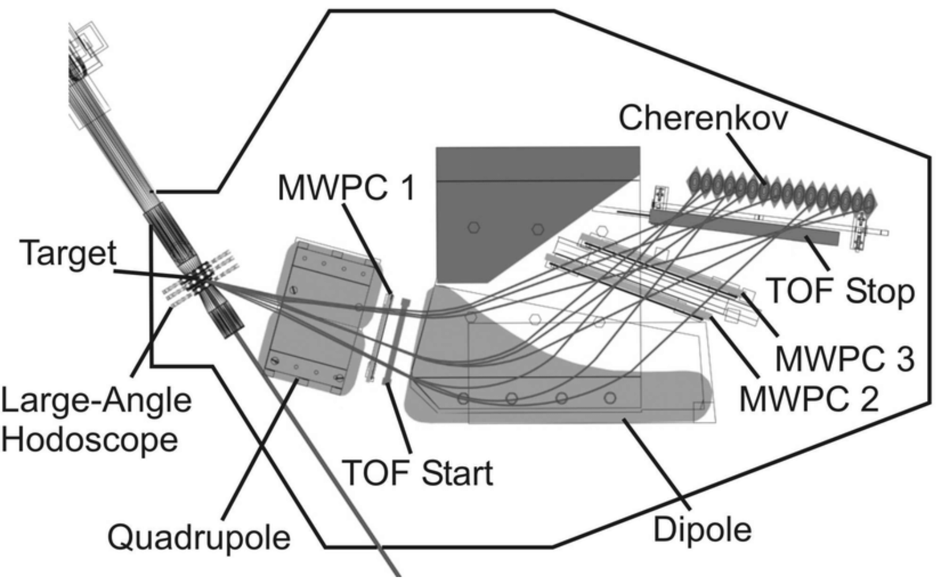

Cherenkov Radiation Threshold Detection - The Kaon Spectrometer

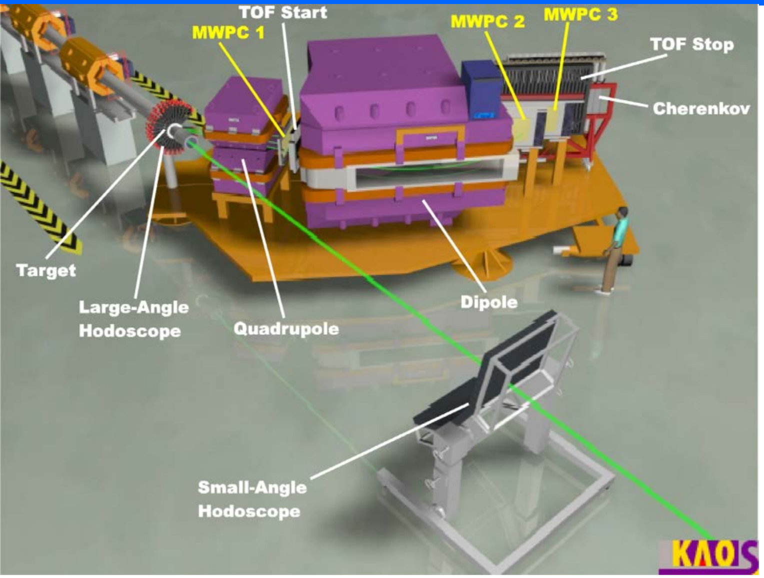

Experimental task is to identify the kaons in a large background of protons and pions.
$p^+, \pi^+, K^+\ rate: \quad \sim 10000/1000/1$

- Time-of-flight (ToF) measurement
- Cherenkov detectors
  1) lucite ($n = 1.49, \beta \geq 0.67$) and water ($n = 1.34, \beta \geq 0.75$) i.e. above the velocity of protons for $p < 0.8\ GeV/c$ and $p < 1\ GeV/c$ respectively
  2) silica aerogel ($n = 1.05, \beta \geq 0.95$) allows separation of pions and kaons

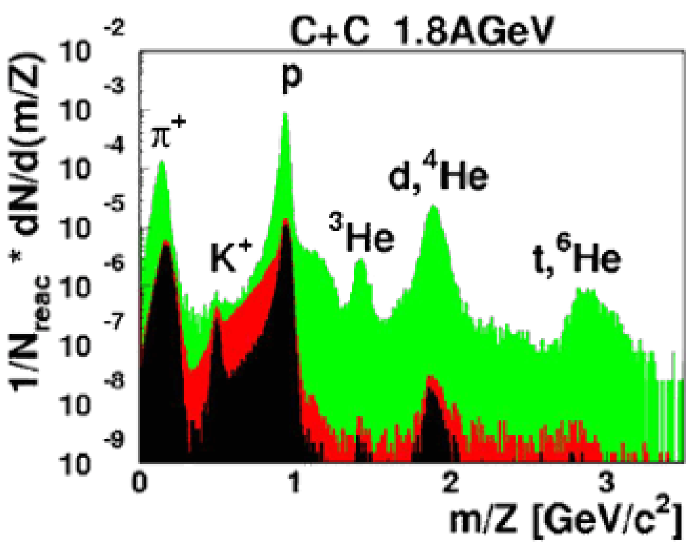

The signal from the plastic ToF-wall in coincidence with the first Cherenkov row and in anti-coincidence with the second one can thus be used as a kaon trigger for momenta above 500 MeV/c.

The **green** spectrum is measured with a trigger on charged particles without ToF.
The **red** one is measured with the ToF trigger.
The **black** spectrum is measured with the kaon trigger.